JVI Journals.ASM.org

Promyelocytic Leukemia Protein Is a Cell-Intrinsic Factor Inhibiting Parvovirus DNA Replication

Angela M. Mitchell,[a,b] Matthew L. Hirsch,[a,c] Chengwen Li,[a,d] R. Jude Samulski[a,e]

Gene Therapy Center, University of North Carolina at Chapel Hill, Chapel Hill, North Carolina, USA[a]; Department of Microbiology and Immunology, University of North Carolina at Chapel Hill, Chapel Hill, North Carolina, USA[b]; Department of Ophthalmology, University of North Carolina at Chapel Hill, Chapel Hill, North Carolina, USA[c]; Department of Pediatrics, University of North Carolina at Chapel Hill, Chapel Hill, North Carolina, USA[d]; Department of Pharmacology, University of North Carolina at Chapel Hill, Chapel Hill, North Carolina, USA[e]

Tripartite motif proteins are important viral restriction factors and affect processes ranging from uncoating to transcription to immune signaling. Specifically, the promyelocytic leukemia protein (TRIM19; also called PML) is a viral restriction factor inhibiting processes from uncoating to transcription to cell survival. Here we investigated PML's effect on adeno-associated virus (AAV), a parvovirus used for gene delivery. Although dependovirus (AAV) and autonomous parvovirus (minute virus of mice) replication centers can colocalize with PML, PML's functional effect on parvoviruses is unknown. Using PML knockout mice, we determined that PML knockout enhances recombinant AAV2 (rAAV2) transduction at a range of vector doses in both male and female mice. In fact, male and female PML knockout mice exhibited up to 56-fold and 28-fold increases in transduction, respectively. PML inhibited several rAAV serotypes, suggesting a conserved mechanism, and organ specificity correlated with PML expression. Mechanistically, PML inhibited rAAV second-strand DNA synthesis, precluding inhibition of self-complementary rAAV, and did not affect the prior steps in transduction. Furthermore, we confirmed the effect of human PML on rAAV transduction through small interfering RNA (siRNA)-mediated knockdown in HuH7 cells and determined that the highest level of inhibition was due to effects of PML isoform II (PMLII). Overexpression of PMLII resulted in inhibition of second-strand synthesis, vector production, and genome replication. Moreover, wild-type AAV2 production and infectivity were also inhibited by PMLII, demonstrating a PML interaction with wild-type AAV. These data have important implications for AAV-mediated gene therapy. Additionally, PMLII inhibition of AAV second-strand synthesis and replication, which are processes necessary for all parvoviruses, suggests implications for replication of other parvoviruses.

Adeno-associated virus (AAV) is a helper-dependent member of the *Parvoviridae* family, which, in addition to AAV, contains other viruses of clinical and veterinary importance, such as B19 parvovirus, human bocavirus, and canine parvovirus. AAV consists of an icosahedral capsid surrounding a single-stranded DNA genome carrying two genes, *Rep* and *Cap*, and has been developed as a gene delivery vector for gene therapy applications. For use as a vector or virus-like particle (recombinant AAV [rAAV]), the viral genes can be removed and replaced with a transgene cassette, with the terminal repeats being the only viral elements required in *cis* (1). Although clinical rAAV-mediated gene therapy has demonstrated increasing success in reaching efficacy goals, especially in restricted sites such as the eye (2), low transgene expression or loss of expression over time has repeatedly compromised efficacy in other clinical trials (3, 4). Therefore, efforts to increase the efficiency of rAAV transduction without increasing the vector dose are imperative.

AAV's replication pathway involves receptor-mediated endocytosis, trafficking to the perinuclear region, nuclear entry, uncoating, and second-strand DNA synthesis, followed by either gene expression or persistence of episomal DNA (reviewed in reference 5). Because AAV evolved to infect cells in the presence of a helper virus, it relies on these viruses, traditionally adenovirus (Ad) or herpes simplex virus (HSV), for various processes in its infection pathway. AAV helper virus functions range from increasing the efficiency of intracellular viral trafficking (6) to inducing AAV gene expression (7) to allowing cell escape (8). In examining AAV biology, rAAV can be utilized to study the steps in AAV production prior to replication, as it undergoes the same transduction steps as wild-type AAV, through second-stand synthesis, but cannot proceed with replication, making AAV a good model for studying the initial transduction of parvoviruses without the later steps of replication occluding the results.

The AAV helper viruses Ad and HSV share the ability to modify or degrade the promyelocytic leukemia protein (PML). PML is a member of the tripartite motif (TRIM) family of proteins, which play a key role in both cell-intrinsic and immune host responses against viruses (reviewed in reference 9). The antiviral mechanisms of TRIM proteins range from that of TRIM5α, which directly binds to incoming HIV-1 capsids, preventing uncoating (10), to that of TRIM21, an intracellular antibody receptor which causes proteasome-mediated degradation of antibody-bound virions (11), to regulation of pattern recognition receptor signaling by at least eight different TRIMs (reviewed in reference 12). PML (TRIM19) is an interferon-responsive protein involved in a wide variety of cellular processes, including apoptosis, differentiation, and antiviral defense. Various isoforms of PML are present in the cytoplasm, nucleoplasm, and PML bodies (13). PML bodies, punctate nuclear structures formed by a lattice of PML protein, act as organizing centers for protein modifications and as depots for

Received 4 October 2013 **Accepted** 29 October 2013
Published ahead of print 6 November 2013
Address correspondence to R. Jude Samulski, rjs@med.unc.edu.
Copyright © 2014, American Society for Microbiology. All Rights Reserved.
doi:10.1128/JVI.02922-13

storage of key cellular proteins (14). PML inhibits infection by many RNA and DNA viruses through a variety of diverse mechanisms. These mechanisms include inhibition of vesicular stomatitis virus and human foamy virus transcription by PML isoform III (15, 16), sequestration of HSV ICP0 in the cytoplasm by PMLIb (17), sequestration of varicella-zoster viral capsids in a cage of PMLIV (18), and activation of p53 and induction of apoptosis by PMLIII in response to poliovirus (19). These mechanisms illustrate the breadth of viral families affected by PML and the range of mechanisms by which they are affected.

To avoid PML antiviral activity, many viruses encode PML-modifying proteins. For instance, Ad E4Orf3 binds directly to PMLII and causes its rearrangement from spherical PML bodies to tract-like structures (20, 21). Furthermore, HSV encodes ICP0, an E3 ligase that causes proteasomal degradation of PML (22–24). In a natural AAV infection, the PML-modifying properties of helper viruses may protect AAV from any potential inhibitory effects of PML. Moreover, not only have AAV replication centers been shown to colocalize with PML tract-like structures in the presence of Ad (25), but the replication centers of an autonomous parvovirus, minute virus of mice (MVM), have also been demonstrated to colocalize with PML bodies during specific times in its replication cycle (26). However, the functional consequences of PML on parvovirus transduction and replication have not been examined. Therefore, we asked whether, in the absence of a helper virus, PML is capable of inhibiting rAAV transduction. To address this question, we utilized PML knockout mice, small interfering RNA (siRNA)-mediated knockdown in human cells, and overexpression of PML isoforms. We demonstrated that PML inhibits the transduction of rAAV both *in vivo* and in human cells in culture. This inhibition is due to the prevention of second-strand synthesis, and the majority of inhibition can be traced to PML isoform II. PMLII can also inhibit the production of both rAAV and wild-type AAV and infection by wild-type AAV. These data may lead to strategies for enhancing the efficiency of rAAV-mediated gene therapy. In addition, these data may have implications for the other members of the parvovirus family.

MATERIALS AND METHODS

Cell culture and virus production. HEK293, HeLa, and HuH7 cells were maintained in Dulbecco's modified Eagle medium (DMEM) supplemented with 10% fetal bovine serum (FBS), 100 U/ml penicillin, and 100 g/ml streptomycin at 37°C with 5% CO_2. Adult mouse tail fibroblasts were cultured in the medium described above supplemented with 1× minimum essential medium (MEM) nonessential amino acids. AAV vectors were produced through cesium gradient purification as described previously (27). Self-complementary rAAV and corresponding control vectors were purified to yield pure virus as described previously (28). Wild-type AAV was produced in the same way as rAAV, except that the plasmid carrying AAV's genes and the transgene cassette plasmid were replaced with pSSV9. Virus and vectors were titrated by quantitative PCR (qPCR) (27).

Isolation of adult mouse tail fibroblasts. Adult tail snip fibroblasts were isolated using a protocol in the ENCODE database (http://genome.ucsc.edu/ENCODE/protocols/cell/mouse/Fibroblast_Stam_protocol.pdf). Briefly, tail snips were clipped into Hanks' balanced salt solution (HBSS; Life Technologies) and minced with a razor blade. The tissue was then digested with collagenase type XI-S at a final concentration of 1,000 U/ml in HBSS for 30 min at 37°C. Tissue was washed once with HBSS, resuspended in 0.05% trypsin-EDTA (Life Technologies), and incubated at 37°C for 20 min. The tissue was then resuspended in complete growth medium, pipetted to dissociate cells, and seeded in 35-mm plates with tissue clumps under glass coverslips. The medium was changed every 4 days. When cells were subcultured, the cells were detached with 0.25% trypsin-EDTA (Life Technologies) and seeded at ratios of 1:2 to 1:4.

Animals and *in vivo* transduction assays. All animal experiments were conducted in accordance with the policies of the Institutional Animal Care and Use Committee at the University of North Carolina at Chapel Hill. Wild-type 129/SV and PML knockout 129/SV-*PML*^{tm1Ppp} mice (29) were a kind gift from Pier Paolo Pandolfi (Beth Israel Deaconess Cancer Center). Age- and sex-matched mice were treated with the indicated rAAV dose in phosphate-buffered saline (PBS) by retro-orbital injection. Transduction from luciferase-encoding vectors was assayed by live luciferase imaging (28). Transduction from green fluorescent protein (GFP) vectors was determined using a GFP enzyme-linked immunosorbent assay (ELISA) kit (Cell Biolabs, Inc.). Briefly, livers were harvested at 7 days posttransduction and minced. A sample (approximately 50 mg) was lysed with RIPA buffer and homogenized with a Tissue-Tearor (BioSpec Products), and the total protein concentration was determined using the Bio-Rad protein assay and a Bio-Rad SmartSpec Plus spectrophotometer. Equal amounts of protein were used to proceed with the GFP ELISA per the manufacturer's directions. A Bio-Rad iMark plate reader was used to determine absorbance, and pg GFP per mg total protein was calculated.

Biodistribution experiments and PML expression analysis. Mice were treated with rAAV as described for transduction experiments, and the specified organs were harvested and frozen on day 14 posttransduction. The organs were minced, and small samples were taken for luciferase assay and vector genome quantification. Luciferase samples were lysed in 2× passive lysis buffer (Promega) and homogenized with a TissueLyser (Qiagen) for 5 min at 40 Hz. The lysate was cleared by centrifugation, and luciferase activity was assayed per the manufacturer's instructions (Promega), using a Wallac1420 Victor2 plate reader. Protein levels were determined as described for transduction assays. Vector genome copy number was determined by harvesting total DNA with a DNeasy Blood and Tissue kit (Qiagen) and performing qPCR with equal volumes of DNA, as described previously (28). For determination of *in vivo* PML expression, the indicated organs were harvested, and 100-mg samples were immediately stored in RNA*later* (Qiagen) at 4°C. RNA was purified with TRIzol (Life Technologies) per the manufacturer's instructions. cDNA was synthesized using a High Capacity cDNA reverse transcription kit (Life Technologies), and transcript levels relative to those of glyceraldehyde-3-phosphate dehydrogenase (GAPDH) were determined by qPCR.

qPCR protocols and primers. To determine PML expression levels from cDNAs made from mouse tissues and from human cells, qPCR assays were designed using the Universal Probe Library Assay Design Center (Roche). The amplicon was designed to be in the 5′ region shared between PML isoforms. For mouse tissues, the primers and probe for PML were as follows: 5′-AGAGGAACCCTCCGAAGACT-3′, 5′-ATTCCTCCTGTATGGCTTGC-3′, and Mouse Universal Probe Library probe 76 (Roche). The primers and probe for mouse GAPDH were as follows: 5′-GGGTTCCTATAAATACGGACTGC-3′, 5′-CCATTTTGTCTACGGGACGA-3′, and Mouse Universal Probe Library probe 52 (Roche). For human cells, the primers and probe for PML were as follows: 5′-TTCTGCTCCAACCCCAAC-3′, 5′-CGCTGATGTCGCACTTGA-3′, and Human Universal Probe Library probe 5 (Roche). The primers and probe for human GAPDH were as follows: 5′-ATCACTGCCACCCAGAAGACT-3′, 5′-ACACGGAAGGCCATGCCA-3′, and Mouse Universal Probe Library probe 34 (Roche). The qPCRs were run with LightCycler 480 Probes master mix (Roche) in a Roche LightCycler 480 machine, using the following program: 95°C for 10 min, 45 cycles of 95°C for 10 s, 60°C for 30 s, and 72°C for 1 s (acquisition), and a final step at 40°C for 30 min. Standard curves for each primer set were used to determine efficiency and to calculate relative expression.

Entry, nuclear fractionation, and DNase protection assays. Mice were treated as described for transduction experiments, and livers were harvested at the indicated time points and placed immediately on ice. Nuclear fractionation and DNase protection assays were performed as

described previously (30), with slight modifications. After mincing, small samples of liver tissue were taken and analyzed for total vector genome copy number as described for biodistribution experiments. Ultracentrifugation through a sucrose cushion was performed for 20 min. Nuclear and DNase-protected DNAs were purified by use of a DNeasy Blood and Tissue kit, with 5 μg salmon sperm DNA (Life Technologies) added to DNase-treated samples to act as a carrier. We determined the purity of isolated nuclei to be >99.5%, using an EnzChek acid phosphatase assay kit (Life Technologies).

siRNA and *in vitro* transduction assays. We used SMARTpool On-TARGETplus PML siRNA (Thermo Scientific) to knock down human PML and On-TARGETplus nontargeting control pool siRNA (Thermo Scientific) as a negative control. HuH7 cells were seeded and transfected with DharmaFECT per the manufacturer's instructions, with slight modifications. HuH7 cells were transfected with 25 nM siRNA 48 h and 24 h prior to transduction. At the time of transduction, the medium was changed to contain the indicated dose of rAAV, and cells were incubated for 24 h. Cells were harvested with 1× passive lysis buffer (Promega), and luciferase and protein assays were performed as described above. Mouse fibroblasts were seeded 16 h prior to transduction, and the medium was changed to contain rAAV at the indicated dose at the time of transduction. Transduction was assayed as described for siRNA experiments, at 48 h posttransduction.

PML isoform plasmid backbone control and PMLII cloning. To generate a pEGFP-C3 backbone plasmid not containing a PML construct, pEGFP-C3-PMLII was digested with BglII and BamHI (New England BioLabs), and the 4.7-kb band was gel purified (Qiagen). This band was self-ligated with T4 DNA ligase (New England BioLabs) and transformed into XL10 Gold ultracompetent cells (Agilent Technologies), and colonies were screened by digestion with AgeI and AvrII (New England BioLabs). To clone the PMLII sequence into the pTR-ss-CMV-EGFP backbone, pTR-ss-CMV-EGFP was digested with SalI (New England BioLabs), and then the ends were blunted with Klenow DNA polymerase (New England BioLabs). The DNA was purified with a PCR purification kit (Qiagen) to remove the enzymes and buffers. The DNA was then digested with AgeI (New England BioLabs), and a 4.2-kb band containing the plasmid backbone without the enhanced GFP (EGFP) gene was gel purified (Qiagen). For retrieval of the PMLII DNA, the pEGFP-C3-PMLII plasmid was PCR amplified with primers 5′-AAACCGGTCCATGGAGCCTGCACC-3′ and 5′-CCCTTCTCTTGTAACCTTGGAATTCGC-3′ and with Illustria RTG Hot Start mix (GE Healthcare). The PCR program was as follows: 95°C for 5 min, 30 cycles of 95°C for 30 s, 60°C for 30 s, and 72°C for 120 s, 72°C for 5 min, and a hold at 4°C. The ends of the PCR product were blunted with Klenow polymerase, PCR purified, and then digested with AgeI. The 2.6-kb PCR product was then gel purified. The fragments were ligated with T4 DNA ligase and transformed into electrocompetent DH10B cells (Life Technologies), and colonies were picked based on sequence.

PML overexpression experiments. GFP-tagged overexpression constructs for PML isoforms I to VI were a kind gift from Peter Hemmerich (Leibniz Institute for Age Research). The backbone plasmid was used as a negative control. HeLa cells were transfected with PML plasmids at a 1:1 ratio with either pTR-CBA-Luc or salmon sperm DNA (Life Technologies). Briefly, HeLa cells were seeded in 24-well plates at 8×10^4 cells per well 24 h prior to transfection. The cells were transfected by use of PEI Max (Polysciences, Inc.) with a 1:1 ratio of the appropriate PML or backbone control plasmid (pEGFP-C3-PMLI, pEGFP-C3-PMLII, pEGFP-C1-PMLIII, pEGFP-C1-PMLIV, pEGFP-C1-PMLV, pEGFP-C1-PMLVI, or pEGFP-C3) and either pTR-CBA-Luc or salmon sperm DNA (Life Technologies). Total amounts used per well were 0.5 μg total DNA and 3 μl PEI Max (1 mg/ml) in 50 μl Opti-MEM (Life Technologies) added to 500 μl complete growth medium. Transfection complexes were incubated for 10 min and then added to cells. Cells were incubated for 16 h, and then the medium was changed to remove transfection reagents. Cells were transduced at 24 h posttransfection. Cells were transduced with 500 vector genomes (vg)/cell rAAV2-CBA-Luc at 24 h posttransfection, incubated for 24 h, and assayed for transduction by luciferase assay. Luciferase values from transduction were normalized to those from transfection. For the self-complementary rAAV experiment, HeLa cells were seeded, transfected with pTR-CMV-PMLII or pTR-CMV-Luciferase and carrier DNA, and transduced with the indicated doses of single-stranded or self-complementary rAAV2-CMV-EGFP at 24 h posttransfection. Transduction was assayed at 24 h by flow cytometry (28).

Virus and vector production assays. For rAAV2 production experiments, HEK293 cells were seeded onto 15-cm plates at a 1:3 density 24 h prior to transfection (for 70% confluence at the time of transfection). For transfection, pXX680 (12 μg/plate), a pXR plasmid (10 μg/plate), and a pTR-CMV plasmid carrying either the PMLII gene or a reporter gene (6 μg/plate) were combined with 520 μl Opti-MEM (Life Technologies) and 110 μl 1-mg/ml PEI Max (Polysciences, Inc.). The complexes were incubated for 10 min at room temperature, and then the total volume was added to the plates and cells were incubated for 48 h to allow vector production. Cells were harvested, vector was purified as described above, and vector was titrated by qPCR. For rAAV2 and wild-type AAV protein level experiments and wild-type AAV production experiments, HEK293 cells were seeded at 1:3 in 10-cm plates 24 h prior to transfection. For rAAV experiments, cells were transfected as described above with 4.8 μg of pXX680, 4 μg of pXR2, and 2.4 μg of either pTR-CMV-Luciferase or pTR-CMV-PMLII in 208 μl Opti-MEM and 44 μl PEI Max. For wild-type AAV2 experiments, cells were transfected as described above with 4.8 μg of pXX680, 4 μg of pSSV9, and 2.4 μg of either pEGFP-C3 or pEGFP-C3-PMLII in 208 μl Opti-MEM and 44 μl PEI Max. Cells were incubated for 48 h to allow production. For wild-type AAV2 production, cells were harvested and DNase treated as for virus production, and titers were measured by qPCR. Immunoblotting was performed as described previously (31), with slight modifications. Samples of 150 μg of protein were loaded on 12% Mini-PROTEAN TGX precast polyacrylamide gels (Bio-Rad) and electrophoresed at 225 V for 35 min in Tris-glycine-SDS buffer (Bio-Rad). Proteins were transferred to a nitrocellulose membrane by use of an iBlot apparatus (Life Technologies) on P3 for 4 min. AAV capsid proteins were detected with B1 antibody, Rep proteins with IF11 antibody, GFP-PML fusion constructs with Santa Cruz Biotech antibody sc-9996, and actin with Abcam antibody ab8226.

Replication and infection assays. For rAAV DNA replication assays, HEK293 cells were seeded at a 1:4 density into 10-cm plates 24 h prior to transfection with PMLII or control plasmid. For transfection, 6 μg of pEGFP-C3 or pEGFP-PMLII was combined with 300 μl DMEM without FBS or antibiotics and 40 μl PEI Max (Polysciences, Inc.) and incubated for 10 min at room temperature. The entire volume was added to the plate, and cells were incubated for 6 h. The medium was then changed to remove the transfection reagents. Three days following transfection of the PML overexpression plasmid or an EGFP expression plasmid, an additional transfection was performed to investigate rAAV replication. Three plasmids were used in this PEI transfection: (i) the adenoviral helper plasmid XX680 (10 μg); (ii) pXR2 (3 μg), which supplies Rep2 and Cap2; and (iii) the AAV vector plasmid (3 μg) pITR2-CBA-luc. Three days following the second transfection, Hirt DNA was isolated using a modified protocol (32) and digested overnight with DpnI (New England BioLabs). Samples were separated in an alkaline gel and transferred to a nitrocellulose membrane (Amersham XL), and hybridization was performed with the product of a random-primed labeling reaction (Roche), using the packaged transgenic DNA sequence as the template (which also served as our size standard) (27). Blots were exposed to film, and DNA quantitation of the replication products was performed using ImageJ.

For wild-type AAV2 infection experiments, HEK293 cells were seeded at 1:3 in 10-cm plates 24 h prior to transfection. The cells were transfected as described before with 3 μg pEGFP-C3 or pEGFP-C3-PMLII and 3 μg pXX680 or salmon sperm DNA in 300 μl Opti-MEM and 40 μl PEI Max. Transfection cocktails were incubated for 10 min at room temperature, and the total volume was added to the plates. The medium was changed to

remove transfection reagents at 6 h posttransfection. At 24 h posttransfection, the cells were concurrently seeded into 24-well plates at 1×10^5 cells/well and infected with the indicated dose of AAV2. Total DNA was harvested at 48 h posttransduction by use of a DNeasy Blood and Tissue kit, and numbers of viral genomes per cell were analyzed by qPCR.

Data analysis. We determined the statistical significance of all data by using the nonparametric Kruskal-Wallis test and considered P values of <0.05 to be significant.

RESULTS

PML knockout enhances rAAV2 transduction *in vivo*. During wild-type AAV's natural life cycle, replicating AAV may be sheltered from the effect of PML by the PML-modifying activity of its helper viruses. We hypothesized that PML may inhibit rAAV transduction in environments where helper viruses are not present. To test this hypothesis, we transduced wild-type (129/SV; $PML^{+/+}$) and PML knockout (129/SV-*PML*^{tm1Ppp}; $PML^{-/-}$) mice with a range of rAAV2-luciferase doses and examined transduction by live imaging. Although we observed very low levels of transduction with 1×10^{10} vg/mouse, we observed expression of luciferase in the area of the liver at day 11 posttransduction in $PML^{-/-}$ mice, whereas no expression was observable in $PML^{+/+}$ mice (Fig. 1A). At a 5-fold higher dose of virus (5×10^{10} vg/mouse), we observed transduction at the site of injection in $PML^{+/+}$ mice, although liver expression was still low; however, liver and injection site expression was apparent in $PML^{-/-}$ mice (Fig. 1B). With 1×10^{11} vg/mouse, a commonly utilized dose of AAV, transduction levels observed in $PML^{+/+}$ mice were similar to those seen with 5×10^{10} vg/mouse; however, $PML^{-/-}$ mice demonstrated increased levels of liver and injection site transduction (Fig. 1C). At a high dose of rAAV2 (5×10^{11} vg/mouse), we observed high levels of transduction in all mice, but there was more transduction in $PML^{-/-}$ mice (Fig. 1D). By quantifying the light output, we observed significant enhancements of transduction in $PML^{-/-}$ mice compared to $PML^{+/+}$ mice at all of the tested doses for either total transduction (Fig. 1E) or transduction in the area of the liver (Fig. 1F), demonstrating that knockout of PML can enhance rAAV2 transduction and suggesting that PML can inhibit rAAV2 transduction.

We performed the AAV dose experiment with female mice. Because male mice have repeatedly been demonstrated to have higher liver transduction levels than female mice (33), we more thoroughly examined the effects of PML knockout in male and female mice to determine whether the higher transduction levels in male mice would override the effects of PML knockout. We transduced male and female $PML^{+/+}$ and $PML^{-/-}$ mice with 2×10^{11} vg/mouse rAAV2 and assayed transduction by live imaging. For female mice, quantification demonstrated significantly enhanced transduction in $PML^{-/-}$ mice at both 7 days and 12 days posttransduction (Fig. 1G). In fact, transduction was 28.2-fold higher at 7 days and 18.6-fold higher at 12 days posttransduction. For male mice, transduction was also significantly higher in $PML^{-/-}$ mice, being 10.8-fold higher at 4 days and 56.4-fold higher at 11 days posttransduction (Fig. 1H). These data demonstrate that PML causes significant inhibition of rAAV2 transduction *in vivo* and that this effect can be observed in both male and female mice.

Effect of PML knockout is conserved among several rAAV serotypes. After determining that PML inhibited rAAV2 transduction *in vivo*, we examined the transduction of various serotypes of rAAV in $PML^{-/-}$ mice to determine whether the transduction pathway affected by PML is specific to rAAV2 or is conserved among rAAV serotypes. Therefore, we transduced $PML^{+/+}$ and $PML^{-/-}$ mice with 1×10^{11} vg/mouse rAAV6, rAAV8, or rAAV9 and assayed transduction by live luciferase imaging. At 7 days posttransduction, we observed enhanced rAAV6 transduction in the area of the liver in $PML^{-/-}$ mice (Fig. 2A) and quantified this enhancement at 15.0-fold (Fig. 2B). In addition, we observed higher transduction from rAAV8 (Fig. 2C) and quantitated this increase at 47.0-fold at 3 days posttransduction (Fig. 2D). At 7 days posttransduction, the luciferase expression in rAAV8-transduced $PML^{-/-}$ mice saturated our imaging capabilities even with very short exposures (data not shown). With rAAV9, we observed increased transduction in $PML^{-/-}$ mice at day 7 posttransduction (Fig. 2E) and quantified this difference at 5.6-fold (Fig. 2F). Thus, these data demonstrate that PML knockout can enhance transduction of a number of rAAV serotypes, suggesting that PML inhibits a process in AAV transduction that is conserved between serotypes.

PML knockout enhances rAAV transduction in a manner correlating to PML expression. To investigate further the enhancement of rAAV transduction we observed in $PML^{-/-}$ mice, we determined in which organs transduction was enhanced by measuring transduction *ex vivo*. We transduced $PML^{-/-}$ and $PML^{+/+}$ mice with rAAV2, harvested organs at 14 days posttransduction, and measured luciferase activity and the vector genome copy number. We observed significant increases in luciferase activity from the liver (22.6-fold) and the kidney (9.2-fold); however, we observed no increase in activity in heart and lung tissues and saw very little muscle transduction (Fig. 3A). In addition, we observed no differences in rAAV2 genome copy number in any of the organs tested (Fig. 3B). Although these data suggest that there may be some organ specificity of the effect of PML on rAAV transduction, rAAV2's strong liver tropism hinders this conclusion. Therefore, we investigated the effect of PML knockout on the biodistribution of rAAV9, a systemic vector (34).

As with rAAV2, we transduced $PML^{-/-}$ and $PML^{+/+}$ mice with rAAV9 and harvested tissues at 14 days posttransduction. Similar to the case with rAAV2, we observed significant increases in luciferase activity in the liver (3.9-fold), spleen (2.8-fold), and kidney (5.2-fold) and no significant increases in heart, lung, and muscle (Fig. 3C). In addition, the only significant changes in vector genome copy number observed were in the liver, where the copy number was 3.5-fold higher in $PML^{-/-}$ mice, and the lung, where the copy number was 2-fold lower in $PML^{-/-}$ mice (Fig. 3D). The smaller transduction enhancement observed with rAAV9 at this time point than that observed with rAAV2 may be due to the much greater transduction efficiency observed with wild-type mice and rAAV9 vectors. To investigate the organ specificity of PML's rAAV transduction enhancement further, we examined the expression of PML in $PML^{+/+}$ mice by quantitative reverse transcription-PCR (qRT-PCR). We observed the highest levels of PML expression in the liver and spleen, intermediate levels of expression in the kidney, low levels of expression in the heart and lung, and very low levels of expression in the muscle (Fig. 3E). Interestingly, we observed no increase in PML expression in the liver following rAAV2 transduction (data not shown), suggesting that rAAV transduction does not induce PML transcription. As the levels of PML expression appear to correlate with the enhancement of rAAV9 transduction in $PML^{-/-}$ mice that we observed (Fig. 3C), this suggests that the organ specificity of the PML enhancement observed occurred based on various PML ex-

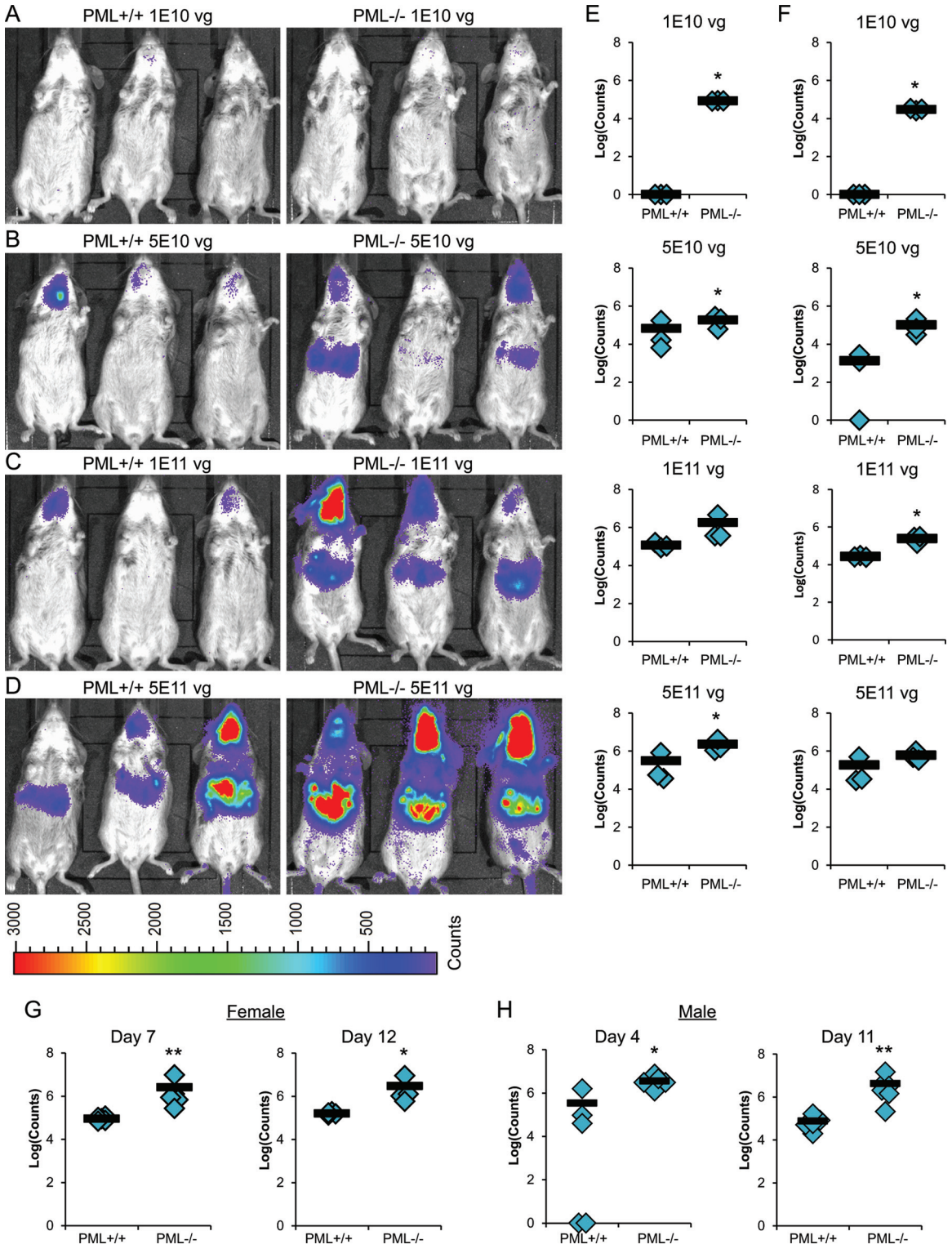

FIG 1 PML knockout enhances rAAV2 transduction at several vector doses in both male and female mice. (A to D) Female $PML^{+/+}$ and $PML^{-/-}$ mice were transduced with 1×10^{10} vg (A), 5×10^{10} vg (B), 1×10^{11} vg (C), or 5×10^{11} vg (D) rAAV2-CBA-luciferase and assayed by live luciferase imaging at 11 days posttransduction (5-min exposure). (E and F) Light output from luciferase live imaging was quantified for either the whole mouse (E) or the area of the liver (F) ($n = 3$). (G and H) Female (G) and male (H) $PML^{+/+}$ and $PML^{-/-}$ mice were transduced with 2×10^{11} vg rAAV2-CBA-luciferase, transduction was assayed by live luciferase imaging at two time points posttransduction, and light output from the whole mouse was quantified (5-min exposures for all, except males on day 11, for which the exposure was 1 min; $n = 5$ for all groups except $PML^{-/-}$ males, for which $n = 6$). Data for individual mice are shown as diamonds, while the bars indicate the means. *, $P < 0.05$; **, $P < 0.01$ versus $PML^{+/+}$ mice.

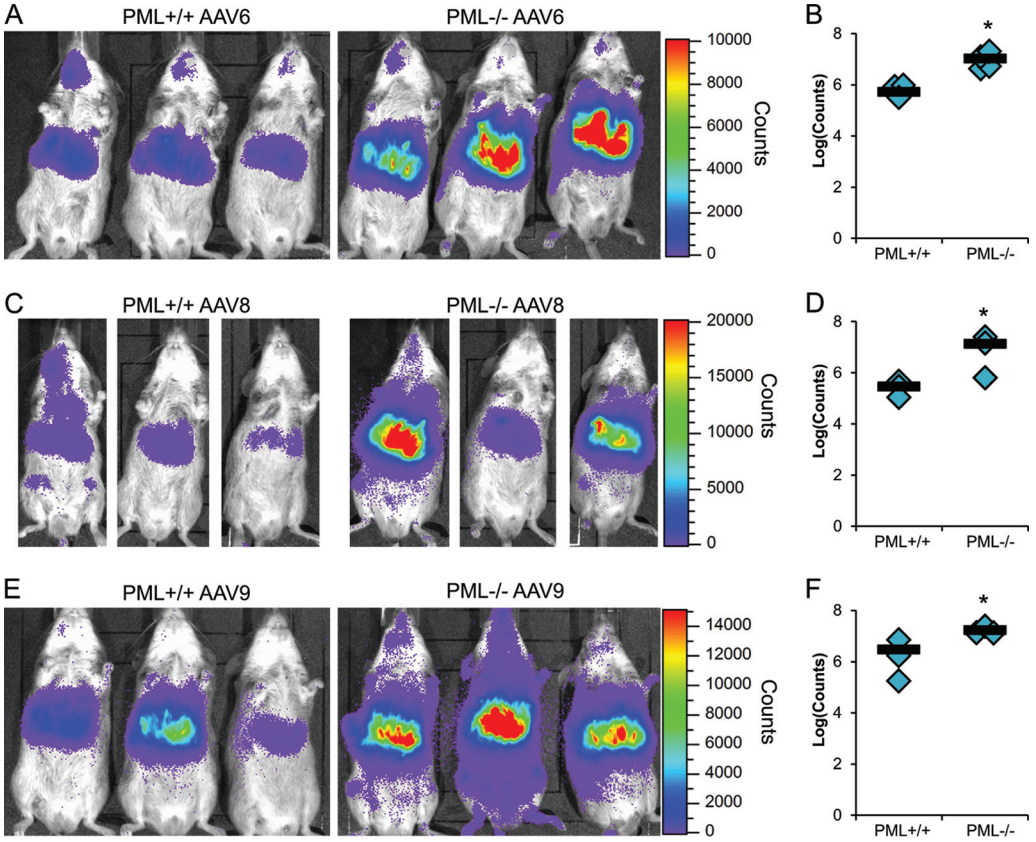

FIG 2 Enhancement of rAAV transduction by PML knockout is conserved among several serotypes. Male $PML^{+/+}$ and $PML^{-/-}$ mice were transduced with 1×10^{11} vg and assayed by live luciferase imaging. (A) Images of mice transduced with rAAV6-CBA-luciferase at 7 days posttransduction (30-s exposure). (B) Quantification of light output from mice in panel A. (C) Images of mice transduced with rAAV8-CBA-luciferase at 3 days posttransduction (30-s exposure). (D) Quantification of light output from mice in panel C. (E) Images of mice transduced with rAAV9-CBA-luciferase at 7 days posttransduction (30-s exposure). (F) Quantification of light output from mice in panel E. Data for individual mice are shown as diamonds, while the bars indicate the means ($n = 3$ for all groups except $PML^{-/-}$ rAAV6-transduced mice, for which $n = 4$). *, $P < 0.05$ versus $PML^{+/+}$ mice.

pression levels. Furthermore, our genome copy number data (Fig. 3B and D) suggest that changes in rAAV genome number are not necessary for PML's effect on rAAV transduction.

PML inhibits rAAV second-strand DNA synthesis. PML is present in both the cytoplasm and nucleoplasm of cells and, additionally, forms PML nuclear bodies that organize posttranslational modification of many proteins (9); therefore, it is possible for PML to affect rAAV transduction directly or indirectly at many transduction steps. To determine the step in rAAV transduction that PML knockout affects, we transduced $PML^{-/-}$ and $PML^{+/+}$ mice with rAAV2 and harvested liver tissue at several times posttransduction. We first asked whether the difference occurred in cell entry by determining the vector genome copy numbers at 1 day and 7 days posttransduction. We observed no difference in copy number between $PML^{+/+}$ and $PML^{-/-}$ mice at either time point (Fig. 4A), suggesting that the effect of PML occurs postentry. This agrees with our biodistribution data demonstrating no difference in rAAV2 vector genome copy number at 14 days posttransduction (Fig. 3B). We next performed nuclear fractionation to determine levels of nuclear entry at these time points. At both 1 day and 7 days, we observed equal numbers of nuclear vector genomes in $PML^{+/+}$ and $PML^{-/-}$ mice (Fig. 4B), suggesting that PML acts after rAAV2 nuclear entry. The next step in rAAV transduction after nuclear entry is uncoating of the vector genome; therefore, we assayed the numbers of uncoated genomes by performing a DNase protection assay on our nuclear fractions. We observed no difference in the numbers of unprotected (uncoated) genomes between $PML^{+/+}$ and $PML^{-/-}$ mice (Fig. 4C), suggesting that PML acts after this transduction step, on either second-strand DNA synthesis or transcription.

To access whether PML knockout affects second-strand DNA synthesis, we transduced $PML^{+/+}$ and $PML^{-/-}$ mice with self-complementary and single-stranded rAAV8-EGFP and determined the transduction in harvested liver tissue at 7 days posttransduction. Self-complementary rAAV genomes do not require second-strand synthesis for transcription and thus should be unaffected by inhibition of this step. As expected, with single-stranded rAAV8, we observed a 7.9-fold transduction enhancement in $PML^{-/-}$ mice; however, we observed no difference in transduction from self-complementary rAAV8 between $PML^{+/+}$ and $PML^{-/-}$ mice (Fig. 5A), suggesting that PML inhibits rAAV second-strand DNA synthesis. To further substantiate this conclusion, we treated fibroblasts from the $PML^{+/+}$ and $PML^{-/-}$ mice with a wide range of rAAV2 doses to determine whether there was a difference in the lower transduction threshold. We hypothesized that transduction increases with PML knockout might be greater at lower vector doses if PML affects second-strand synthesis, as annealing of genomes could not compensate

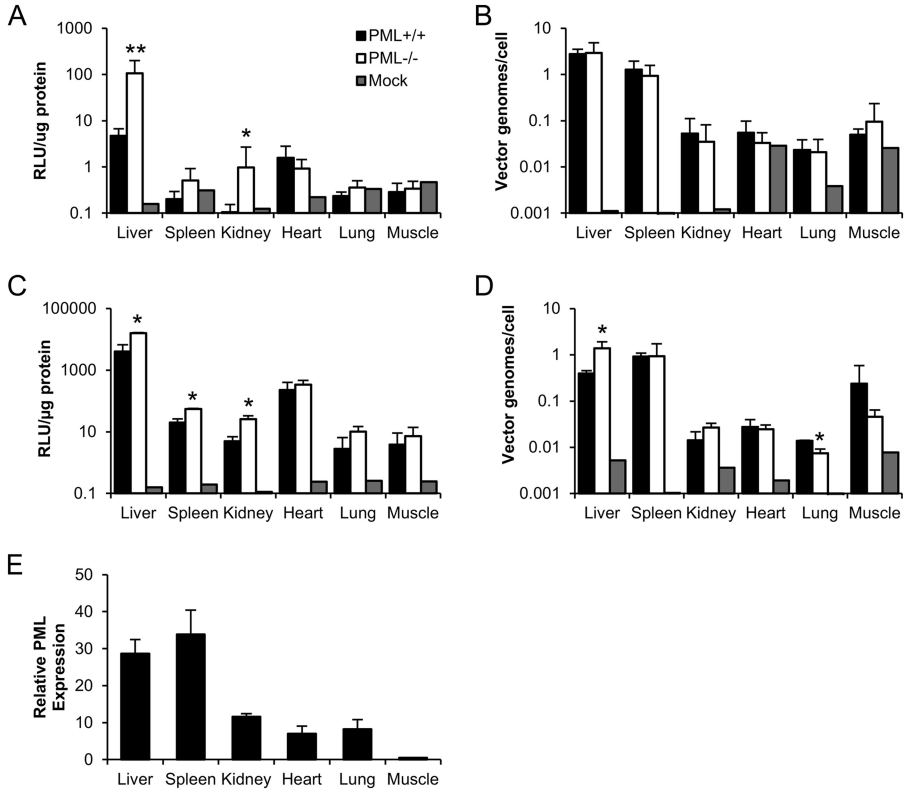

FIG 3 rAAV transduction enhancement is organ specific and correlates with PML expression. (A and B) PML$^{+/+}$ and PML$^{-/-}$ female mice were transduced with 2×10^{11} vg rAAV2-CBA-luciferase, and the indicated organs were harvested at 14 days posttransduction. Tissue was assayed for luciferase activity (A) and vector genome copy number (vg/cell) ($n = 5$) (B). Gray bars indicate the average values for two untransduced female mice. (C and D) PML$^{+/+}$ and PML$^{-/-}$ male mice were transduced with 1×10^{11} vg rAAV9-CBA-luciferase, and the indicated organs were harvested at 14 days posttransduction. Tissue was assayed for luciferase activity (C) and vg/cell ($n = 3$) (D). Gray bars indicate values for an untransduced mouse. (E) The indicated organs were harvested from untransduced male PML$^{+/+}$ mice, and RNA was purified. PML expression relative to that of GAPDH was determined by qRT-PCR ($n = 3$). Values are given as means with 1 standard deviation (SD). RLU, relative light units. *, $P < 0.05$; **, $P < 0.01$ versus PML$^{+/+}$ mice.

for a lack of second-strand synthesis. In fact, we observed transduction in the 100-vg/cell group for PML$^{-/-}$ cells but did not observe transduction in the PML$^{+/+}$ cells until the 500-vg/cell group (Fig. 5B), demonstrating a lower threshold for transduction in PML$^{-/-}$ cells. These data also agree with our *in vivo* dosing data showing a similar threshold at our lowest rAAV2 dose (Fig. 1A). The differences in the threshold for transduction support our mechanism of PML inhibition of rAAV second-strand DNA synthesis. Taken together, our results demonstrate that PML knockout enhances second-strand DNA synthesis of rAAV vectors, suggesting that PML can inhibit this transduction step.

Human PML inhibits rAAV transduction through the actions of PMLII. Our data to this point demonstrate the effect of murine PML knockout on rAAV transduction. To confirm the validity of our results for human PML, we used siRNA to knock down PML in HuH7 cells, a hepatocellular carcinoma cell line, and achieved 68% knockdown on an RNA level (data not shown). We transduced cells with several doses of rAAV2-luciferase and determined that knockdown approximately doubled rAAV2 transduction at all doses tested (Fig. 6A). Although this increase is less than that observed *in vivo*, it is similar to that achieved in primary fibroblasts harvested from mice at the higher vector doses (Fig. 5B). Therefore, incomplete knockdown (data not shown) and differences between *in vitro* and *in vivo* environments likely account for the smaller effect of knockdown. Nevertheless, these data confirm that human PML can inhibit rAAV transduction. Human PML has at least seven major isoforms and a number of minor isoforms, all of which share their N-terminal domains and differ in their C-terminal domains (9). Of the major isoforms, isoforms I through VI are nuclear (13) and could possibly mediate the effect of PML on rAAV2 second-strand synthesis. We acquired plasmids expressing EGFP-tagged versions of these nuclear isoforms (35), expressed them in HeLa cells (Fig. 6B), and examined the effects of these isoforms on rAAV2 transduction. We determine that expression of five of the six isoforms (PMLI, PMLIII, PMLIV, PMLV, and PMLVI) resulted in an approximately 2-fold decrease in transduction, while expression of PMLII resulted in a 4.9-fold decrease in transduction (Fig. 6C). This greater effect of PMLII than those of the other isoforms cannot be explained by their relative levels of protein accumulation (Fig. 6B). To confirm our *in vivo* mechanism, we then examined whether PMLII could inhibit self-complementary rAAV2 transduction. In fact, although we observed a significant decrease in the number of cells transduced with single-stranded rAAV2 after PMLII overexpression, we observed significantly less inhibition of self-complementary rAAV2 transduction (Fig. 6D), confirming that human PML isoform II is responsible for the inhibition of rAAV second-strand synthesis.

PMLII overexpression inhibits rAAV2 and wild-type AAV2 production and replication. All of our data thus far addressed the

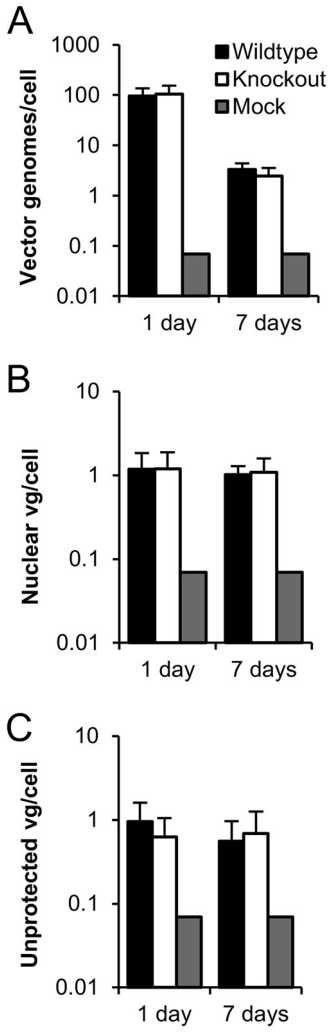

FIG 4 PML does not inhibit rAAV cell entry, nuclear localization, or uncoating. (A to C) $PML^{+/+}$ and $PML^{-/-}$ female mice were transduced with 1×10^{11} vg rAAV2-CBA-luciferase, and livers were harvested at the indicated times posttransduction. (A) Total numbers of vg/cell were measured by qPCR ($n = 5$). (B) Nuclei were isolated by subcellular fractionation, and numbers of nuclear vg/cell were measured by qPCR ($n = 5$). (C) Nuclei were DNase digested to completion, and numbers of remaining vg were determined. Numbers of unprotected vg/cell were calculated ($n = 5$). Gray bars indicate values for untransduced mice ($n = 2$). Values are given as means and 1 SD.

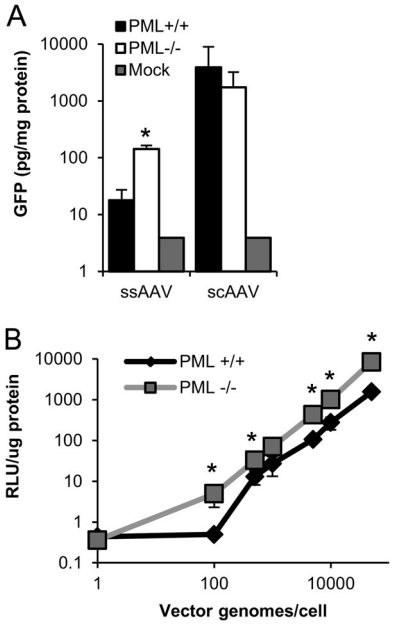

FIG 5 PML inhibits rAAV second-strand DNA synthesis. (A) $PML^{+/+}$ and $PML^{-/-}$ female mice were transduced with 1×10^{11} vg single-stranded rAAV8-CMV-GFP (ssAAV) or self-complementary rAAV8-CMV-GFP (scAAV), and livers were harvested at 7 days posttransduction. Transduction was determined by GFP ELISA ($n = 3$). Gray bars indicate values for an untransduced mouse. (B) Adult mouse tail fibroblasts from $PML^{+/+}$ and $PML^{-/-}$ mice were transduced with the indicated doses of rAAV2-CBA-luciferase and assayed at 48 h by normalized luciferase assay. Fibroblast data represent three independent experiments. Values are given as means and 1 SD. *, $P < 0.05$ versus $PML^{+/+}$ mice.

role of PML in rAAV transduction; however, given our second-strand synthesis mechanism, we set out to determine whether PML plays a role in rAAV genome replication and virus production. We began by examining the effect of PMLII overexpression on virus production by encoding PMLII from a transgene in rAAV vectors. We determine that the presence of the PMLII transgene resulted in a 6.8-fold decrease in the yield of vector (Fig. 7A). As the effect of PML on rAAV transduction was through second-stand synthesis, we hypothesized that PMLII inhibits rAAV production on the level of genome replication. Therefore, we performed a replication assay to determine whether the level of replicated DNA was lower in cells expressing PMLII than in cells expressing a control vector. In fact, we observed slightly lower levels of the replicative monomer and dimer forms of the vector genome in PMLII-expressing cells (Fig. 7B), which were quantified at 73% of the control value (Fig. 7C). We then examined whether PML could also inhibit the production of wild-type AAV by producing wild-type AAV2 from an infectious clone, with or without PMLII overexpression, and assaying the levels of virus produced. As with rAAV2, we observed a 6.5-fold decrease in wild-type AAV2 when PMLII was overexpressed (Fig. 7D), demonstrating that PML also inhibits wild-type AAV2. We further investigated this production effect with both wild-type and recombinant AAV by examining levels of the Rep and capsid proteins. We observed greatly reduced levels of all three capsid proteins, as well as the four Rep proteins, with PMLII overexpression (Fig. 7E), although the degree of decrease varied. These data demonstrate that PML can inhibit the production of both recombinant and wild-type AAV on the protein level. Because utilizing an infectious clone of AAV2 avoids the initial steps of AAV's infectious pathway and introduces high levels of template for the viral genome, we then tested the effect of PMLII overexpression on the infection of wild-type AAV by transfecting cells with PMLII and the Ad helper plasmid, infecting them with AAV2, and determining the number of viral genomes produced. At 48 h postinfection, we observed a large, significant inhibition of AAV2 replication in the presence of PMLII (Fig. 7F), especially at low viral doses (60.1-fold at 1 vg/cell and 1,207-fold at 0.1 vg/cell). We also observed significant inhibition of AAV2 infection by PMLII at earlier time points (data not shown), confirming PML's inhibitory role in AAV's life cycle. Overall, our results demonstrate that PML can inhibit the transduction of rAAV vectors in both human and murine contexts through the inhibition of second-strand DNA syn-

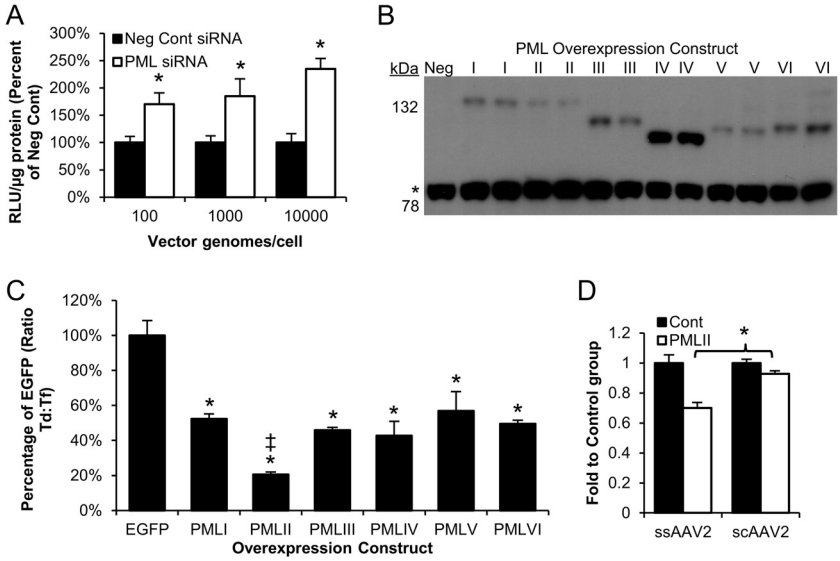

FIG 6 Human PML, especially isoform II, inhibits rAAV transduction and second-strand synthesis. (A) HuH7 cells were transfected with PML or negative-control siRNA 48 and 24 h prior to transduction with rAAV2-CBA-luciferase at the indicated dose. Transduction was assayed by luciferase assay at 24 h posttransduction. Values are given as percentages of the negative-control value (Neg Cont) for the vector dose. (B) HeLa cells were transfected with the indicated PML overexpression construct, and expression was analyzed by immunoblot analysis at 24 h posttransfection. GFP-PML fusion proteins were detected using a GFP antibody. Constructs are shown in duplicate. Neg, nontransfected cells. The asterisk indicates a cellular band serving as a loading control. (C) HeLa cells were transfected with the indicated PML overexpression or control plasmid 24 h prior to transduction with 500 vg/cell rAAV2-CBA-luciferase. Transduction was assayed by luciferase assay at 24 h posttransduction and normalized to the value from transfection (Td:Tf). Values are given as percentages of the control construct value. (D) HeLa cells were transfected with PMLII or control plasmid 24 h prior to transduction with either 1,000 vg/cell single-stranded rAAV2-CMV-EGFP (ssAAV2) or 200 vg/cell self-complementary rAAV2-CMV-EGFP (scAAV2). At 24 h posttransduction, cells were assayed by flow cytometry. Values given are percentages of cells transduced as fold values over that for the control plasmid group. Data represent three independent experiments. Values are given as means and 1 SD. *, $P < 0.05$ versus control; ‡, $P < 0.05$ versus other isoforms.

thesis. Moreover, we traced this inhibition to human PMLII and expanded the effect to the production of recombinant and wild-type AAV and to wild-type AAV infectivity.

DISCUSSION

In this study, we examined the functional role of PML in the transduction of AAV and in AAV production and infection in order to determine whether PML can inhibit AAV. We determined that PML inhibits rAAV transduction *in vivo* in a manner that correlates with the PML expression level and that is conserved among serotypes. Utilizing subcellular fractionation as well as self-complementary rAAV, we demonstrated that the inhibition of rAAV transduction by PML appears to occur at the level of conversion of the single-stranded vector genome to a functional double-stranded form. In addition, we established that human PML, especially PMLII, can also inhibit rAAV2 transduction and production and wild-type AAV2 infection. To our knowledge, these data represent the first time that a functional role for PML in the transduction or replication of a parvovirus has been described.

Four pieces of data contribute to our conclusion that PML inhibits rAAV second-strand DNA synthesis. (i) Equal numbers of vector genomes completed the pre-second-strand synthesis transduction steps of cell entry, nuclear entry, or uncoating *in vivo* in $PML^{+/+}$ and $PML^{-/-}$ mice. (ii) Neither PML knockout *in vivo* nor PML knockdown in human cells had an effect on self-complementary rAAV transduction, which avoids second-strand synthesis by self-annealing. (iii) Both *in vitro* and *in vivo* dose-response curves demonstrated that a lower threshold rAAV dose was required for successful transduction with $PML^{-/-}$ mice, suggesting a greater effect of PML at low vector doses where possible annealing of vector genomes cannot compensate for a lack of second-strand synthesis. (iv) Our rAAV DNA replication assay demonstrated a small but significant decrease in rAAV genome replication when PML was overexpressed. Taken together, these data provide strong evidence suggesting inhibition of rAAV second-strand DNA synthesis by PML. Interestingly, in examining rAAV9 biodistribution, we observed an increase in vector genome copy number with PML knockout specifically in the liver. Although this apparent increase may be due to the very high transduction efficiency of rAAV9 allowing a change in vector genome copy number due to second-strand synthesis, this will require further investigation in the future.

PML affects the replication of many viruses through sequestration of viral components (17, 18) or prevention of transcription (15, 16); however, we are not aware of any other studies demonstrating a PML effect specifically on genome replication. AAV genome replication relies on the cellular replication machinery, including DNA polymerase δ, replication factor C, proliferating cell nuclear antigen, and replication protein A (RPA) (36, 37), although second-strand synthesis has not been examined directly. In the future, it will be interesting to investigate whether any of these factors are involved in PML's effect on rAAV second-strand synthesis. Interestingly, RPA, through association with RPA interacting protein β (RIPβ), is sequestered by PML (38); however, we could find no evidence of a role for RPA in the inhibition of rAAV transduction by PML (data not shown). We also could not observe a direct interaction between PML and rAAV genomes or capsids (data not shown). Resources such as a manually curated PML

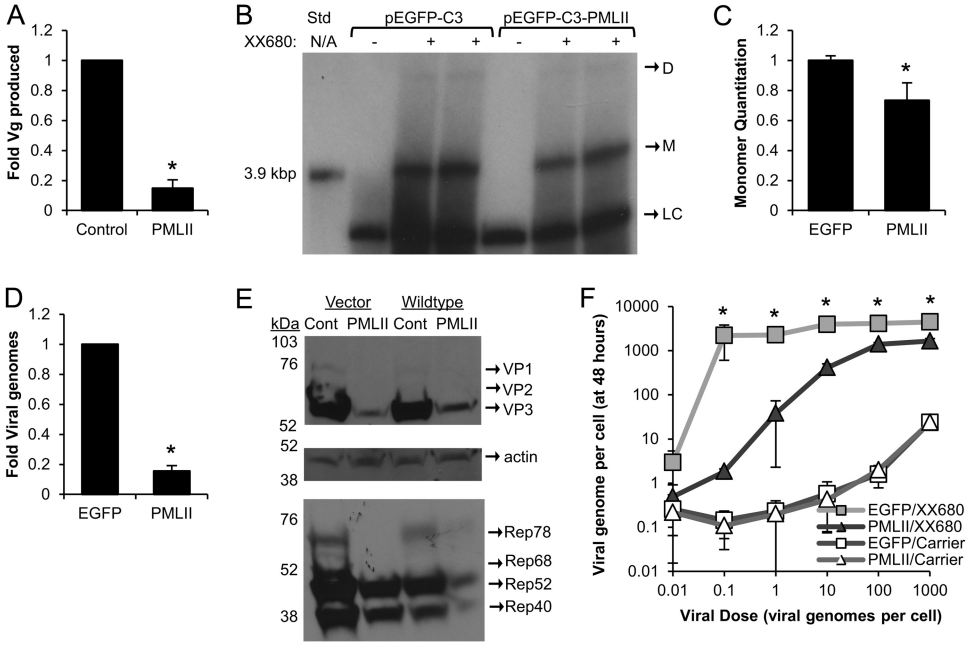

FIG 7 Production and replication of rAAV and AAV2 are inhibited by PMLII. (A) HEK293 cells were transfected for production of vector carrying either the PMLII gene or a control gene (i.e., luciferase or EGFP gene). At 48 h posttransfection, vector was harvested and purified. The amount of vector produced was determined by qPCR. Values indicate mean fold changes compared to the control transgene for three separate vector preparations, with standard errors of the means (SEM). (B) HEK293 cells were transfected with PMLII or control plasmid 24 prior to transfection with viral production plasmids. At 72 h posttransduction, small-molecular-weight DNA was harvested. Replicative forms of rAAV DNA were detected by Southern blotting. No pXX680 lanes represent negative controls for replication. M, monomer; D, dimer; LC, loading control (DpnI-digested plasmid). The image is representative of three trials on two blots. (C) Monomer bands from the three trials for panel B were quantified by densitometry. Values given are means and 1 SD. (D) HEK293 cells were transfected with PMLII or control plasmid (pXX680) and an AAV2 infectious clone. At 48 h posttransfection, virus was harvested and production was assayed by qPCR. Values indicate mean fold changes compared to the control transgene for three separate vector preparations, with SEM. (E) HEK293 cells were treated as in panel A for vector groups and as in panel D for virus groups. Protein was harvested at 48 h, and AAV capsid proteins (VP1, VP2, and VP3) and nonstructural proteins (Rep78, Rep68, Rep52, and Rep40) were assayed by immunoblotting. Actin served as a loading control. The blot is representative of three independent experiments. (F) HEK293 cells were transfected with pXX680 or carrier DNA and the PMLII or control plasmid 24 h prior to infection with the indicated dose of AAV2. AAV genome copy number was determined by qPCR at 48 h postinfection. Data represent three independent experiments. Values given are means ± 1 SD. *, $P < 0.05$ versus control.

interactome (39) should facilitate the identification of factors through which PML acts on rAAV transduction, as well as the mechanism of PML's effect. Moreover, as the same replication factors are involved in MVM DNA replication as in AAV DNA replication (40) and PML overexpression greatly inhibited AAV2 replication, it will be interesting to determine whether PML plays a role in the second-strand synthesis and DNA replication of other parvoviruses.

In addition to investigating the role of PML in rAAV transduction *in vivo*, we examined the effect of human PML on AAV in order to eliminate the possibility that the PML effects were specific to mice and determined that human PML could also inhibit rAAV transduction. Furthermore, given that PML acted at a nuclear step in transduction, we examined the six major nuclear human PML isoforms and elucidated their effects on rAAV. We determined that overexpression of five of the isoforms (I, III, IV, V, and VI) caused a 2-fold decrease in rAAV2 transduction, while PMLII caused a 5-fold decrease in transduction. Two possible hypotheses could explain the partial effect of several isoforms and full effect of one isoform: (i) PML proteins contain two domains important for rAAV transduction inhibition, including one in the shared exons (1 to 7a) and one in the unique region of PMLII; or (ii) the effect on rAAV transduction is unique to PMLII, and overexpression of other isoforms draws more endogenous PMLII into PML bodies (35), where rAAV effects might occur. Further studies will determine which of these hypotheses is correct. Nevertheless, our data clearly demonstrate that PMLII, and specifically its unique region, is important for rAAV transduction inhibition.

The unique region of PMLII consists of the majority of exon 7b and spans amino acids 571 to 824, i.e., the C terminus. Interestingly, while PMLI and PMLII are the most abundant PML isoforms, the majority of known PMLII functions are interactions with AAV's helper viruses Ad and HSV. Specifically, Ad E4Orf3 binds within amino acids 645 to 674 of PMLII and rearranges it to form tract-like structures (21). In addition, the conserved region 3 on Ad E1A-13S interacts with PMLII and may enhance viral and cellular transcription (41). Furthermore, HSV has two distinct mechanisms to decrease PMLII levels: ICP27-induced alternate splicing (42) and degradation of PML by ICP0 (24). In fact, PMLII expression decreases the replication of ICP0 null HSV (43). From these studies, it is clear that PMLII plays an important role in DNA virus replication that is still being elucidated. Further studies with AAV may clarify the role of PML in both DNA virus replication and other cellular processes.

Beyond rAAV transduction, we examined the effect of PML on the production of rAAV and the production and infection of wild-type AAV2. We observed similar decreases in production of wild-type and recombinant AAV with PMLII overexpression and cor-

related this production defect with a small decrease in rAAV DNA replication and a large decrease in viral protein levels. This inhibition of AAV replication by PML raises the question of the role of helper virus functions that affect PML in the replication of AAV. Ad E4Orf3 binds to and rearranges PMLII (20, 21), while HSV ICP0 causes proteasomal degradation of PML (22–24). Although the PML-modifying activities of these proteins have not been shown to provide helper virus functions (44), examining their effects in the context of PML overexpression and in liver-derived cell lines will be interesting in the future. In addition, with the complicated regulation of AAV expression (45–49), it is unclear whether the decrease in protein levels results from the decrease in replication or an addition effect on the viral promoters. Given the known effects of PML on viral transcription (15, 16), the act of PML repressing AAV's promoters would not be unprecedented. We are currently further investigating the roles of genome replication and viral promoter activity in PML's effect. Additionally, we are investigating reversing this phenotype by knocking down PML and possibly increasing vector yields, which would significantly influence rAAV's clinical applications.

In summary, we have demonstrated for the first time that PML inhibits rAAV transduction *in vivo* through inhibition of second-strand DNA synthesis. In addition, we demonstrated that human PML can also inhibit rAAV2 transduction and production and that PMLII is responsible for the majority of this effect. PMLII inhibits wild-type AAV2 production and infection as well. Given the large *in vivo* effect of PML on rAAV transduction, rAAV's interaction with PML will be important to target with rational vector design as this pathway becomes better understood. Designing vectors that avoid PML interactions could lead to large increases in transduction, facilitating systemic gene therapy approaches. In conclusion, pursuing the interaction of AAV with PML may have important implications for understanding AAV biology, clinical vector production, enhancement of rAAV transduction, and understanding the biology of other parvoviruses.

ACKNOWLEDGMENTS

This work was supported by National Institutes of Health grants 1R01AI080726 and 5R01DK084033 (to C.L. and R.J.S.), 5R01AI072176 and 1R01AR064369 (to M.L.H. and R.J.S.), and 1P01HL112761 and 5U54AR056953 (to R.J.S.), as well as fellowship 5T32-AI007419 (to A.M.M.).

We thank the members of the UNC Gene Therapy Center for productive discussions, particularly Sarah Nicolson and Jayme Warischalk. We also thank Sophia Shih for performing qPCR for titration of AAV, biodistribution, and expression experiments. We used equipment and software from the UNC Flow Cytometry Core and the UNC Small Animal Imaging Facility in this study.

REFERENCES

1. **Xiao X, Xiao W, Li J, Samulski RJ.** 1997. A novel 165-base-pair terminal repeat sequence is the sole cis requirement for the adeno-associated virus life cycle. J. Virol. **71:**941–948.
2. **Simonelli F, Maguire AM, Testa F, Pierce EA, Mingozzi F, Bennicelli JL, Rossi S, Marshall K, Banfi S, Surace EM, Sun J, Redmond TM, Zhu X, Shindler KS, Ying G-S, Ziviello C, Acerra C, Wright JF, McDonnell JW, High KA, Bennett J, Auricchio A.** 2010. Gene therapy for Leber's congenital amaurosis is safe and effective through 1.5 years after vector administration. Mol. Ther. **18:**643–650. http://dx.doi.org/10.1038/mt.2009.277.
3. **Manno CS, Pierce GF, Arruda VR, Glader B, Ragni M, Rasko JJ, Ozelo MC, Hoots K, Blatt P, Konkle B, Dake M, Kaye R, Razavi M, Zajko A, Zehnder J, Rustagi PK, Nakai H, Chew A, Leonard D, Wright JF, Lessard RR, Sommer JM, Tigges M, Sabatino D, Luk A, Jiang H, Mingozzi F, Couto L, Ertl HC, High KA, Kay MA.** 2006. Successful transduction of liver in hemophilia by AAV-factor IX and limitations imposed by the host immune response. Nat. Med. **12:**342–347. http://dx.doi.org/10.1038/nm1358.
4. **Nathwani AC, Tuddenham EG, Rangarajan S, Rosales C, McIntosh J, Linch DC, Chowdary P, Riddell A, Pie AJ, Harrington C, O'Beirne J, Smith K, Pasi J, Glader B, Rustagi P, Ng CY, Kay MA, Zhou J, Spence Y, Morton CL, Allay J, Coleman J, Sleep S, Cunningham JM, Srivastava D, Basner-Tschakarjan E, Mingozzi F, High KA, Gray JT, Reiss UM, Nienhuis AW, Davidoff AM.** 2011. Adenovirus-associated virus vector-mediated gene transfer in hemophilia B. N. Engl. J. Med. **365:**2357–2365. http://dx.doi.org/10.1056/NEJMoa1108046.
5. **Mitchell AM, Nicolson SC, Warischalk JK, Samulski RJ.** 2010. AAV's anatomy: roadmap for optimizing vectors for translational success. Curr. Gene Ther. **10:**319–340. http://dx.doi.org/10.2174/156652310793180706.
6. **Xiao W, Warrington KH, Jr, Hearing P, Hughes J, Muzyczka N.** 2002. Adenovirus-facilitated nuclear translocation of adeno-associated virus type 2. J. Virol. **76:**11505–11517. http://dx.doi.org/10.1128/JVI.76.22.11505-11517.2002.
7. **Shi Y, Seto E, Chang LS, Shenk T.** 1991. Transcriptional repression by YY1, a human GLI-Kruppel-related protein, and relief of repression by adenovirus E1A protein. Cell **67:**377–388. http://dx.doi.org/10.1016/0092-8674(91)90189-6.
8. **Geoffroy M-C, Salvetti A.** 2005. Helper functions required for wild type and recombinant adeno-associated virus growth. Curr. Gene Ther. **5:**265–271. http://dx.doi.org/10.2174/1566523054064977.
9. **Geoffroy MC, Chelbi-Alix MK.** 2011. Role of promyelocytic leukemia protein in host antiviral defense. J. Interferon Cytokine Res. **31:**145–158. http://dx.doi.org/10.1089/jir.2010.0111.
10. **Diaz-Griffero F, Qin XR, Hayashi F, Kigawa T, Finzi A, Sarnak Z, Lienlaf M, Yokoyama S, Sodroski J.** 2009. A B-box 2 surface patch important for TRIM5alpha self-association, capsid binding avidity, and retrovirus restriction. J. Virol. **83:**10737–10751. http://dx.doi.org/10.1128/JVI.01307-09.
11. **Mallery DL, McEwan WA, Bidgood SR, Towers GJ, Johnson CM, James LC.** 2010. Antibodies mediate intracellular immunity through tripartite motif-containing 21 (TRIM21). Proc. Natl. Acad. Sci. U. S. A. **107:**19985–19990. http://dx.doi.org/10.1073/pnas.1014074107.
12. **McNab FW, Rajsbaum R, Stoye JP, O'Garra A.** 2011. Tripartite-motif proteins and innate immune regulation. Curr. Opin. Immunol. **23:**46–56. http://dx.doi.org/10.1016/j.coi.2010.10.021.
13. **Condemine W, Takahashi Y, Zhu J, Puvion-Dutilleul F, Guegan S, Janin A, de The H.** 2006. Characterization of endogenous human promyelocytic leukemia isoforms. Cancer Res. **66:**6192–6198. http://dx.doi.org/10.1158/0008-5472.CAN-05-3792.
14. **Lang M, Jegou T, Chung I, Richter K, Munch S, Udvarhelyi A, Cremer C, Hemmerich P, Engelhardt J, Hell SW, Rippe K.** 2010. Three-dimensional organization of promyelocytic leukemia nuclear bodies. J. Cell Sci. **123:**392–400. http://dx.doi.org/10.1242/jcs.053496.
15. **Chelbi-Alix MK, Quignon F, Pelicano L, Koken MH, de The H.** 1998. Resistance to virus infection conferred by the interferon-induced promyelocytic leukemia protein. J. Virol. **72:**1043–1051.
16. **Regad T, Saib A, Lallemand-Breitenbach V, Pandolfi PP, de The H, Chelbi-Alix MK.** 2001. PML mediates the interferon-induced antiviral state against a complex retrovirus via its association with the viral transactivator. EMBO J. **20:**3495–3505. http://dx.doi.org/10.1093/emboj/20.13.3495.
17. **McNally BA, Trgovcich J, Maul GG, Liu Y, Zheng P.** 2008. A role for cytoplasmic PML in cellular resistance to viral infection. PLoS One **3:**e2277. http://dx.doi.org/10.1371/journal.pone.0002277.
18. **Reichelt M, Wang L, Sommer M, Perrino J, Nour AM, Sen N, Baiker A, Zerboni L, Arvin AM.** 2011. Entrapment of viral capsids in nuclear PML cages is an intrinsic antiviral host defense against varicella-zoster virus. PLoS Pathog. **7:**e1001266. http://dx.doi.org/10.1371/journal.ppat.1001266.
19. **Pampin M, Simonin Y, Blondel B, Percherancier Y, Chelbi-Alix MK.** 2006. Cross talk between PML and p53 during poliovirus infection: implications for antiviral defense. J. Virol. **80:**8582–8592. http://dx.doi.org/10.1128/JVI.00031-06.
20. **Doucas V, Ishov AM, Romo A, Juguilon H, Weitzman MD, Evans RM, Maul GG.** 1996. Adenovirus replication is coupled with the dynamic properties of the PML nuclear structure. Genes Dev. **10:**196–207. http://dx.doi.org/10.1101/gad.10.2.196.
21. **Leppard KN, Emmott E, Cortese MS, Rich T.** 2009. Adenovirus type 5 E4

Orf3 protein targets promyelocytic leukaemia (PML) protein nuclear domains for disruption via a sequence in PML isoform II that is predicted as a protein interaction site by bioinformatic analysis. J. Gen. Virol. **90:**95–104. http://dx.doi.org/10.1099/vir.0.005512-0.
22. **Everett RD, Maul GG.** 1994. HSV-1 IE protein Vmw110 causes redistribution of PML. EMBO J. **13:**5062–5069.
23. **Maul GG, Everett RD.** 1994. The nuclear location of PML, a cellular member of the C3HC4 zinc-binding domain protein family, is rearranged during herpes simplex virus infection by the C3HC4 viral protein ICP0. J. Gen. Virol. **75:**1223–1233. http://dx.doi.org/10.1099/0022-1317-75-6-1223.
24. **Everett RD, Parada C, Gripon P, Sirma H, Orr A.** 2008. Replication of ICP0-null mutant herpes simplex virus type 1 is restricted by both PML and Sp100. J. Virol. **82:**2661–2672. http://dx.doi.org/10.1128/JVI.02308-07.
25. **Fraefel C, Bittermann AG, Bueler H, Heid I, Bachi T, Ackermann M.** 2004. Spatial and temporal organization of adeno-associated virus DNA replication in live cells. J. Virol. **78:**389–398. http://dx.doi.org/10.1128/JVI.78.1.389-398.2004.
26. **Young PJ, Jensen KT, Burger LR, Pintel DJ, Lorson CL.** 2002. Minute virus of mice NS1 interacts with the SMN protein, and they colocalize in novel nuclear bodies induced by parvovirus infection. J. Virol. **76:**3892–3904. http://dx.doi.org/10.1128/JVI.76.8.3892-3904.2002.
27. **Grieger JC, Choi VW, Samulski RJ.** 2006. Production and characterization of adeno-associated viral vectors. Nat. Protoc. **1:**1412–1428. http://dx.doi.org/10.1038/nprot.2006.207.
28. **Mitchell AM, Li C, Samulski RJ.** 2013. Arsenic trioxide stabilizes accumulations of adeno-associated virus virions at the perinuclear region, increasing transduction in vitro and in vivo. J. Virol. **87:**4571–4583. http://dx.doi.org/10.1128/JVI.03443-12.
29. **Wang ZG, Delva L, Gaboli M, Rivi R, Giorgio M, Cordon-Cardo C, Grosveld F, Pandolfi PP.** 1998. Role of PML in cell growth and the retinoic acid pathway. Science **279:**1547–1551. http://dx.doi.org/10.1126/science.279.5356.1547.
30. **Thomas CE, Storm TA, Huang Z, Kay MA.** 2004. Rapid uncoating of vector genomes is the key to efficient liver transduction with pseudotyped adeno-associated virus vectors. J. Virol. **78:**3110–3122. http://dx.doi.org/10.1128/JVI.78.6.3110-3122.2004.
31. **Johnson JS, Samulski RJ.** 2009. Enhancement of adeno-associated virus infection by mobilizing capsids into and out of the nucleolus. J. Virol. **83:**2632–2644. http://dx.doi.org/10.1128/JVI.02309-08.
32. **Arad U.** 1998. Modified Hirt procedure for rapid purification of extrachromosomal DNA from mammalian cells. Biotechniques **24:**760–762.
33. **Davidoff AM, Ng CY, Zhou J, Spence Y, Nathwani AC.** 2003. Sex significantly influences transduction of murine liver by recombinant adeno-associated viral vectors through an androgen-dependent pathway. Blood **102:**480–488. http://dx.doi.org/10.1182/blood-2002-09-2889.
34. **Zincarelli C, Soltys S, Rengo G, Rabinowitz JE.** 2008. Analysis of AAV serotypes 1–9 mediated gene expression and tropism in mice after systemic injection. Mol. Ther. **16:**1073–1080. http://dx.doi.org/10.1038/mt.2008.76.
35. **Weidtkamp-Peters S, Lenser T, Negorev D, Gerstner N, Hofmann TG, Schwanitz G, Hoischen C, Maul G, Dittrich P, Hemmerich P.** 2008. Dynamics of component exchange at PML nuclear bodies. J. Cell Sci. **121:**2731–2743. http://dx.doi.org/10.1242/jcs.031922.
36. **Nash K, Chen W, McDonald WF, Zhou X, Muzyczka N.** 2007. Purification of host cell enzymes involved in adeno-associated virus DNA replication. J. Virol. **81:**5777–5787. http://dx.doi.org/10.1128/JVI.02651-06.
37. **Ni TH, McDonald WF, Zolotukhin I, Melendy T, Waga S, Stillman B, Muzyczka N.** 1998. Cellular proteins required for adeno-associated virus DNA replication in the absence of adenovirus coinfection. J. Virol. **72:**2777–2787.
38. **Park J, Seo T, Kim H, Choe J.** 2005. Sumoylation of the novel protein hRIPβ is involved in replication protein A deposition in PML nuclear bodies. Mol. Cell. Biol. **25:**8202–8214. http://dx.doi.org/10.1128/MCB.25.18.8202-8214.2005.
39. **Van Damme E, Laukens K, Dang TH, Van Ostade X.** 2010. A manually curated network of the PML nuclear body interactome reveals an important role for PML-NBs in SUMOylation dynamics. Int. J. Biol. Sci. **6:**51–67. http://dx.doi.org/10.7150/ijbs.6.51.
40. **Christensen J, Tattersall P.** 2002. Parvovirus initiator protein NS1 and RPA coordinate replication fork progression in a reconstituted DNA replication system. J. Virol. **76:**6518–6531. http://dx.doi.org/10.1128/JVI.76.13.6518-6531.2002.
41. **Berscheminski J, Groitl P, Dobner T, Wimmer P, Schreiner S.** 2013. The adenoviral oncogene E1A-13S interacts with a specific isoform of the tumor suppressor PML to enhance viral transcription. J. Virol. **87:**965–977. http://dx.doi.org/10.1128/JVI.02023-12.
42. **Nojima T, Oshiro-Ideue T, Nakanoya H, Kawamura H, Morimoto T, Kawaguchi Y, Kataoka N, Hagiwara M.** 2009. Herpesvirus protein ICP27 switches PML isoform by altering mRNA splicing. Nucleic Acids Res. **37:**6515–6527. http://dx.doi.org/10.1093/nar/gkp633.
43. **Cuchet D, Sykes A, Nicolas A, Orr A, Murray J, Sirma H, Heeren J, Bartelt A, Everett RD.** 2011. PML isoforms I and II participate in PML-dependent restriction of HSV-1 replication. J. Cell Sci. **124:**280–291. http://dx.doi.org/10.1242/jcs.075390.
44. **Geoffroy MC, Epstein AL, Toublanc E, Moullier P, Salvetti A.** 2004. Herpes simplex virus type 1 ICP0 protein mediates activation of adeno-associated virus type 2 rep gene expression from a latent integrated form. J. Virol. **78:**10977–10986. http://dx.doi.org/10.1128/JVI.78.20.10977-10986.2004.
45. **Beaton A, Palumbo P, Berns KI.** 1989. Expression from the adeno-associated virus p5 and p19 promoters is negatively regulated in trans by the rep protein. J. Virol. **63:**4450–4454.
46. **Chang LS, Shi Y, Shenk T.** 1989. Adeno-associated virus P5 promoter contains an adenovirus E1A-inducible element and a binding site for the major late transcription factor. J. Virol. **63:**3479–3488.
47. **Hermonat PL, Santin AD, Batchu RB, Zhan D.** 1998. The adeno-associated virus Rep78 major regulatory protein binds the cellular TATA-binding protein in vitro and in vivo. Virology **245:**120–127. http://dx.doi.org/10.1006/viro.1998.9144.
48. **Pereira DJ, McCarty DM, Muzyczka N.** 1997. The adeno-associated virus (AAV) Rep protein acts as both a repressor and an activator to regulate AAV transcription during a productive infection. J. Virol. **71:**1079–1088.
49. **Weger S, Wendland M, Kleinschmidt JA, Heilbronn R.** 1999. The adeno-associated virus type 2 regulatory proteins rep78 and rep68 interact with the transcriptional coactivator PC4. J. Virol. **73:**260–269.